PELVIC BEHAVIOR IN SIDE COLLISIONS: STATIC AND DYNAMIC TESTS ON ISOLATED PELVIC BONES

Hervé Guillemot
Claude Got
CEESAR, European Center of Safety and Risk Analysis
Benoit Besnault
François Lavaste
Laboratory of Biomechanics, ENSAM Paris
Stéphane Robin
Jean Yves Le Coz
Laboratory of Accidentology and Biomechanics, PSA-Renault
Jean-Pierre Lassau
Laboratory of Anatomy, Faculté des Saint-Pères, Paris
France
Paper Number 98-S6-W-37

ABSTRACT

Car manufacturers are more and more concerned with the protection of the occupants in lateral impacts. Field accident analysis dealing with automotive side collisions suggest that the pelvis is very vulnerable, but there is a lack of knowledge of the behavior of the pelvic bony structure and of its biomechanical tolerance. This knowledge however is essential in order to optimize protection devices and car structures with regard to the security of the occupants.

An experimental study of the pelvic bony structure subjected to static and dynamic loads was carried out in order to document its biomechanical behavior and its injury threshold. 22 pelves were tested under side loading conditions. Displacements, applied force, and local strains of the pubic rami were obtained.

From this study, the main conclusions drawn out were:

- A good agreement is observed between the real life observations and those coming from the in-vitro tests.
- Static fracture threshold is lower in this study than those reported for whole body tests, but is closed to Cesari static results.
- The dynamic fracture threshold is well bordered by the chosen energy level of impact, and consequently, a first corridor including the behavior of the pelvic bony structure up to the level of injury is proposed.

INTRODUCTION

Side collisions represent 15 to 20% of the automotive crashes in which at least one of the occupants was injured but are the cause of 25 to 30% of serious and fatal injuries encountered in all car accidents. The real world crash investigations dealing with lateral impact suggest that the pelvis is very vulnerable. The protection of the occupants in the case of lateral impact is becoming one of the main concerns of the car manufacturers. The optimization of protection devices and car structures still remains difficult to achieve taking into account the behavior of the human body. Since many papers were published dealing with the mechanical behavior of the pelvis, few data are currently available on the behavior of the pelvis, particularly for the isolated bone. The results of the present study thus aim at a better understanding of the pelvis mechanical behavior. This knowledge is of importance in order to design improved crash dummies or mathematical models of the car occupants.

An experimental protocol was thus set up in order to reproduce the injuries observed in real life. Ten isolated pelvic bones were first tested with a static machine, in order to study the overall behavior of the bone structure, and to determine the fracture threshold. Then, dynamic tests were also conducted on isolated pelves. 12 pelves were tested under side loading conditions, using a drop tower with an energy of 30 Joules, this energy level having been determined from the static fracture threshold. The pelves were thus impacted with a falling mass of 3.68 kg at a speed of 4 m/s. Displacement, accelerations, impact force and local strains on the pubic rami were obtained. The fractures observed during those tests were coherent with those observed in real life. Ramus fractures, pelvic ring disruption, or posterior injuries such as sacral fracture were observed. For two dynamic tests, no fractures were obtained, suggesting that the impact conditions were well chosen in order to assess the rupture threshold of the pelvis. Furthermore, other parameters were obtained, such as the geometrical and some histological characteristics of the tested pelves, in order to correlate them with the observed behavior of the specimens.

METHODOLOGY

Several authors described PMHS tests to study the tolerance and the behavior of the pelvic area in side impacts. They consisted essentially in the whole body subjected to lateral impacts. A high variety of means was used, as well as a wide range of mass and impact speed. Sled tests were first described by Melvin [17], Kallieris [12], and Marcus [16]. Recently, Cavanaugh [3] and Zhu [29] presented a series of 17 cadaver tests. Impactor tests were also realized by Cesari [4-6,22], Nuscholtz [19-21], Viano [28], and Chamouard [2]. Finally, Tarriere [27] carried out whole body tests using a drop tower.

On the other hand, tests on isolated pelvic bone were rarely described in the literature. Cesari presented four static tests on hemi pelves [5], and Scales provided data for a F.E. model presented by Plummer [22]. This knowledge is however more and more necessary to design, provide parameters, and validate mathematical models of the pelvis, without taking into account the soft tissues.

Before setting up an experimental protocol, an examination of real life injuries is needed, essentially to insure us that the test produced fractures are in good agreement with those sustained in real crashes.

In a previous study [10], a field accident analysis was carried out to determine precisely the panel of typical injuries observed at the level of the pelvic area in side collisions. A series of 219 occupants and 381 injuries AIS 2+ [1] from the LAB accident database was retained. The main advantage of this database is its ability to provide both medical description and accident circumstances. All the cases were studied, including those involving low mass cars, trucks and fixed obstacles. The pelvic area injuries sustained in side impacts were selected. Pelvic bone fractures, femoral fractures, and low abdomen injuries were included. Thus, a complete examination was realized for the area comprised between the mid abdomen and the mid thigh.

The pelvic fractures were most frequently found (184), followed by the femur fracture (56), and soft tissue injuries (106). By order of importance (Figure 1), pubic fractures were first found (above 50% of all injuries), then femur fractures (25%, from which 75% of diaphysis), acetabular fracture (12%) and posterior fractures, such as sacro-iliac joint and sacral fractures (11%). Pelvic content injuries consisted essentially in retroperitoneal hemorrhages (10%).

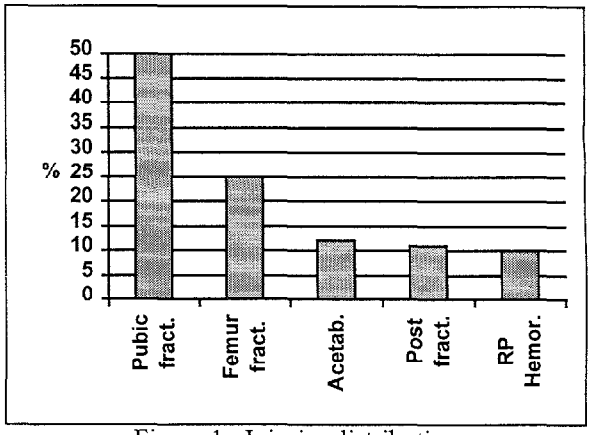

Figure 1 : Injuries distribution

This analysis, focused on injuries selected on the pelvic region, is consistent with other available data [7,8,11,13,15,18].

STATIC TESTS

The typical pelvic injuries were well identify through the previous accident analysis. The following step of this study consisted in a series of static tests, in order to access the overall behavior of the bony structure, the pelvic ring deflexion and the strains at sites of a high probability of fractures.

A reliable loading and a good stability are required for the immobilization of each pelvis. An easily reproduced position, based on standard anatomic landmarks, is also necessary. The positioning was chosen to insure stability and to get most of the bone structure free when subjected to the load. The line between the two anterior superior iliac spines was oriented vertically, corresponding to the Y-axis (Figure 2).

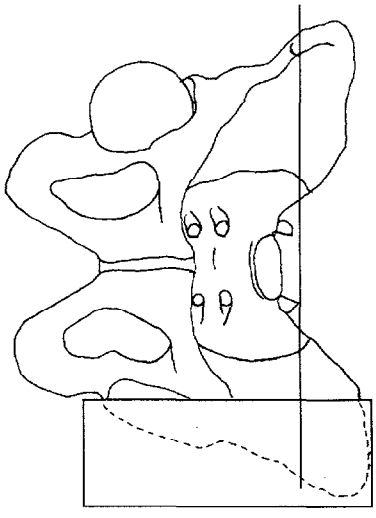

Figure 2 : Anterior view

Therefore, each pelvis was placed in a metallic box and cast with a low melting temperature alloy (< 60° C), the Cerrobend®, up to the external edge of the left ischial tuberosity. Thus, the pelvic ring and the pubic rami were totally free in this configuration. These boundary conditions were chosen because they could be easily reproduced in a finite element model.

The force applied to the pelvis was recorded from a load cell. Six transducers were used to measure the displacements of two points of the pelvic bone according to the reference system defined on Figure 3. The point "A" is situated at the right anterior inferior iliac spine, while point "B" is the superior edge of the pubic symphisis. Two plastic balls were screwed into the bone to materialize these two anatomical points.

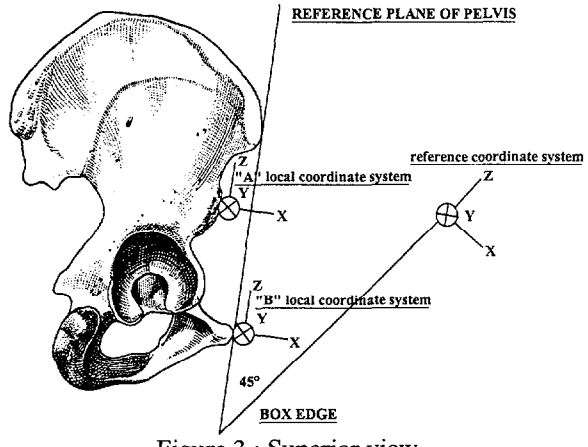

Figure 3 : Superior view

Eight strain gages were glued on each side of the four pubic rami. A ninth gage was placed on the internal side of the iliac wing, 1 cm above the sacro iliac joint. These points were determined by the usual location of fractures (Figure 4).

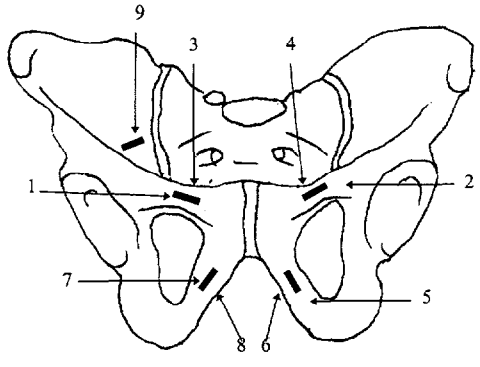

Figure 4 : location of strain gages and A & B points

10 pelvic bones were tested. They were provided from fresh cadavers through the department of anatomy of the "Faculté des Saints Pères" in Paris. Nine of them were male specimen. The age range from 47 to 86 (mean 67 years). Metastasis or a long period of bed rest did not damage the specimens chosen, except for one of them. One of them was frozen and no more data were available. Their principal characteristics are reported in Appendix 1.

Before testing, all the pelves were weighed, and their volumes determined by simple methods, so that their density can be calculated. Several measures were also taken, such as maximum width, diameter of the pelvic ring, and distance between iliac spines. In order to document as accurately as possible the geometry of the tested specimens, a geometrical acquisition was carried out on each tested pelvis using a 3D-measuring device. The measuring protocol was designed in order to provide a classification of the pelves in accordance with the work of Reynolds [26]. Thus, a library of 105 points was acquired.

Each pelvis sustained 3 kinds of tests, at a speed of 5 mm/mn, with an Inströn testing machine. A vertical load (Y direction) was first applied to the right iliac crest, increasing to a maximum of 500 N then returning to 0. Subsequently, the right acetabulum was loaded with a metallic sphere fitted to its diameter up to 500 N then down to 0. Finally, the last test involved increasing the load through the acetabulum until fracture occurred. X rays were taken to confirm and locate fractures. Three types of data are available: displacements, strains, and stiffness via a force displacement curve.

RESULTS

The iliac tests were characterized by effort-displacement curves with a high range in terms of Y displacement of the iliac wing. Responses varied from 1.6 mm to 11.8 mm for a loading of 500 N. The highest value was observed for the female specimen, for which the geometry was quite different (Figure 5). Perpendicular displacements were also measured, of the same order of magnitude as those in the loading direction.

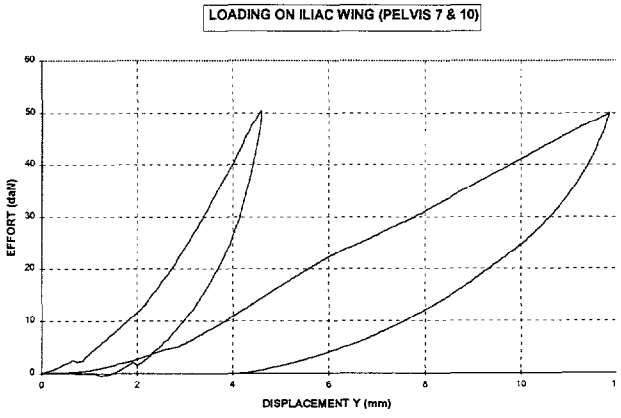

Figure 5 : Force Displacement curves of 7th & 10th Pelvis

Pubic symphisis exhibited lower displacements, from 0.1 to 2.7 mm for the Y direction (Figure 6). Perpendicular values did not exceed 1.2 mm for X & Z directions, except for the female pelvis (2.2 & 2.5 mm). Complete data are reported in Appendix 2.

Point	AIIS			PS		
Direction	dX	dY	dZ	dX	dY	dZ
Min (mm)	0.2	1.6	2.1	0.1	0.1	-0.2
Max (mm)	3.6	11.8	10.8	2.2	2.7	2.5
Mean (n=10)	1.5	4.4	4.2	0.5	0.7	0.6

Table 1 : Displacements on Anterior Inferior Iliac Spine (A) and Pubic Symphisis (B) for 500 N

Displacements observed from the acetabular tests are lower than those of the iliac loading, and range only from 1.2 to 2.5 mm. The 3D analysis of the displacements shows that the deformation pattern of the structure is complex. Coupled movements of the same order of magnitude as those in the loading direction (+Y) are also observed (Figure 7), in the posterior anterior (+X) and vertical (-Z) directions. Complete data are reported in Appendix 3.

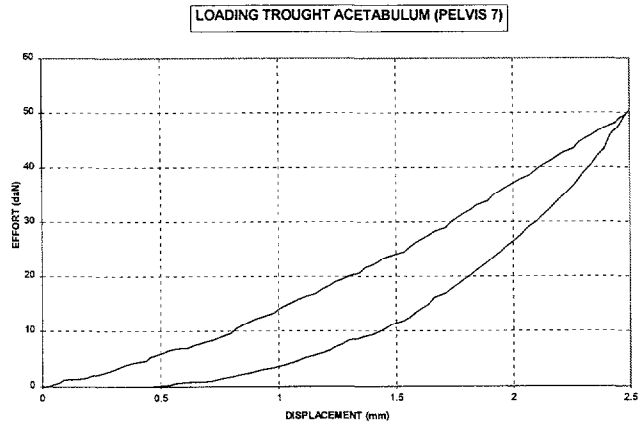

Figure 6 : Force Displacement curves of Pelvis 7

Point	AIIS			PS		
Direction	dX	dY	dZ	dX	dY	dZ
Min (mm)	0.3	1.2	-2.1	0.4	0.4	-1
Max (mm)	2.4	2.5	-0.4	1.6	1.8	0.3
Mean (n=10)	1	1.7	-1.1	0.9	0.9	-0.4

Table 2 : Displacements on Anterior Inferior Iliac Spine (A) and Pubic Symphisis (B) for 500 N

The pubic symphisis exhibits a displacement in the same direction as those of the acetabulum, but of half the magnitude (Figure 8). Finally, one can see that the highest displacement at the level of the pubic symphisis is often observed in the posterior anterior direction.

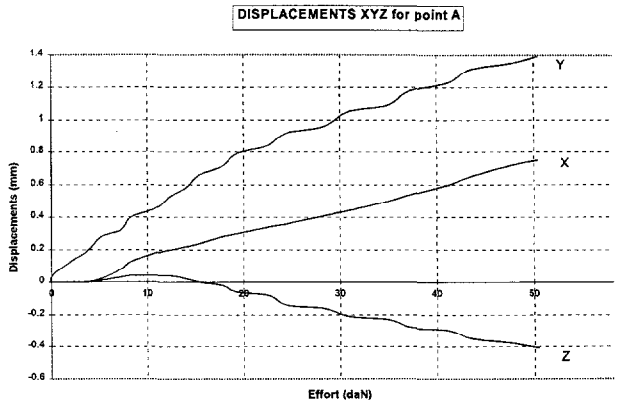

Figure 7 : Displacement curves for Ant Inf. Iliac Spine

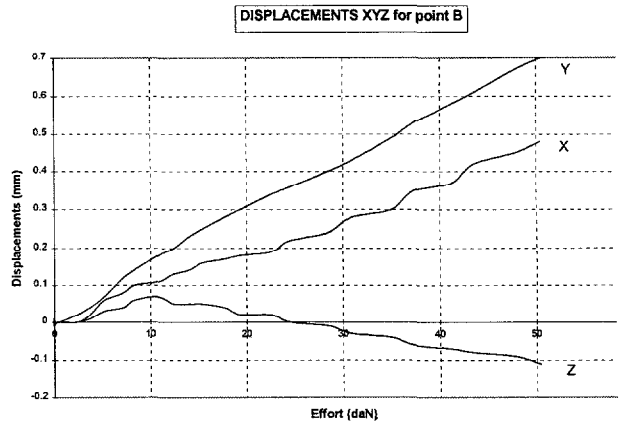

Figure 8 : Displacement curves for Pubic Symphisis

Strain gages

As far as the strains are concerned, it can be noted that all external pelvic strains measured negative values (compression) while all internal pelvic strains are positive (traction). This observation can be related to the postero-anterior displacement of the pubic symphisis. A symmetrical distribution of the stresses can be observed for the two ilio pubic rami, which was not found for the ischio pubic rami.

The following curves (Figure 9) from fracture tests show the behavior of the 10 pelves loaded through acetabulum. Fracture occurs for maximum forces ranging from 1100 to 3450 N (mean 1750 N), and for displacements ranging only from 3.5 to 7.5 mm (mean 5.2 mm). The highest displacement for the pubic symphisis was often observed for the posterior anterior direction, particularly before the fracture occurred.

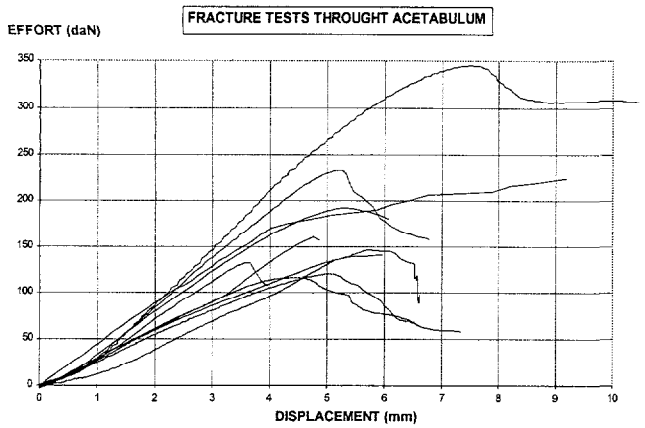

Figure 9 : Force-displacement curves from fracture tests

The load displacement curves enable the computation of a "pseudo-stiffness" of the structure, defined as the ratio between the load and the corresponding displacement (slope of the curve). The results of the tests show a significant difference between the stiffness computed for the load on the acetabulum (denoted Ka), and the pseudo stiffness for the load on the iliac wing (denoted Ki). The greatest ratio between Ka and Ki was found for the female specimen (pelvis 7), for which displacements of the iliac wing were the highest. The others pelves exhibited ratios from 1/2 to 1/3.

	S01	S02	S03	S04	S05	S06	S07	S08	S09	S10
Acetabulum	403	254	416	423	337	249	201	227	231	333
Iliac Wing	206	129	211	206	155	72	46	88	141	105

Table 3 : Stiffness Comparison (N/mm)

DYNAMIC TESTS

The first results, together with a few computer simulations, enabled us to estimate the loading energy necessary to obtain an injury. Nevertheless, the dynamic behavior of the pelvis is not well known when the pelvis is subjected to an impact. A new series of 12 pelves was carried out to access the biomechanical characteristics of the pelvic bone, without soft tissues or pelvic content. Thus, 12 isolated pelves were tested under side loading conditions, using a drop tower with an energy of 30 Joules. The positioning of each pelvis was previously described for static loads, and applied in a same manner for the dynamic procedure (Figure 2). The energy level was determined from static fracture thresholds. The pelves were thus impacted with a falling mass of 3.68 kg at a speed of 4 m/s.

A drop tower was used for these tests (Figure 10). It consisted of a falling mass guided between two rails which enables impact speed around 4 m/s.

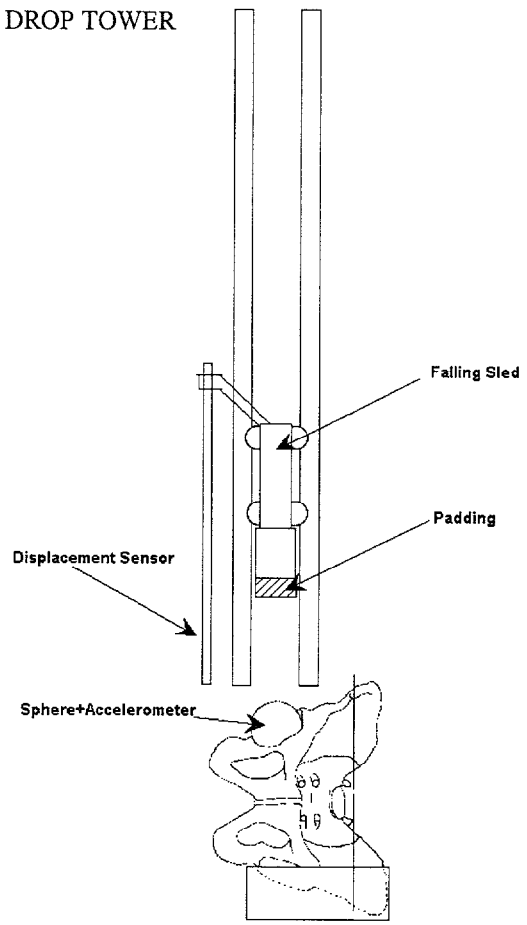

Figure 10 : Schematic view of the testing set-up.

The falling mass was fitted with two accelerometers, the first one to calculate acceleration, force and displacement during the impact. The second one was used to determine precisely the impact speed. A good correlation was found between these two sensor values at the moment of the impact.

A displacement sensor was also used to measure the pelvis deflection.

A metallic ball was fitted into the right acetabulum, to distribute the load on the whole joint surface. Its diameter was chosen by the preliminary geometric measurements. An accelerometer was included in this sphere to know its kinematics and calculate the force applied to the acetabulum. At the time of first impact, only the impacting mass and the impacted sphere were involved, and the high peak force, due to the contact, did not reflect the biomechanics of the pelvis. Thus the applied force was computed from both the falling mass

accelerometer and the sphere accelerometer, as follows (Figure 11):

$$F_y = M_{mass} \times acc_{mass} + M_{sphere} \times acc_{sphere}$$

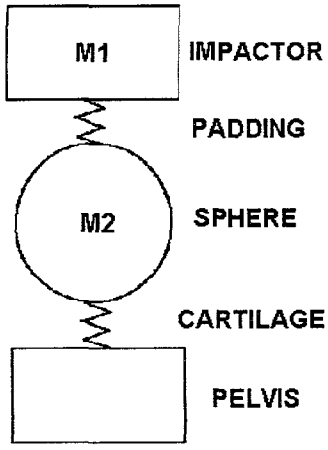

Figure 11 : simplified model of the experimental set-up

To avoid direct contact between two metallic surfaces, a 11-mm thick silicon padding was set at the inferior side of the falling mass. The deflection of this silicon padding was calculated and reached 82 % of its thickness. This padding played the role of a physical filter and thus the raw data were used for the accelerometers. So, direct measurement by displacement sensor cannot be used. But, another advantage of using this internal accelerometer is to calculate directly the deflection by integrating twice the signal. So this data can be used to establish behavior curves.

This experimental set-up was verified by several tests on a padding surface, which was calculated to simulate the behavior of a human pelvis, in terms of acceleration and displacement. The results obtained are illustrated by the following figure (Figure 12).

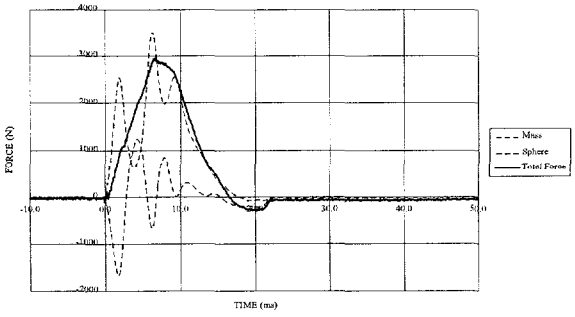

Figure 12 : Impact force with the experimental model

In addition, four strain gages were glued on the external side of each pubic ramus (Figure 13). The number of gages was reduced compared to those used for static tests, because information provided for internal and external sides of the same ramus was redundant. These strain gages were oriented along the main axis of the ramus. They were not used to measure stress precisely, but to compare the behavior of one ramus to the others. Nevertheless, they can be used to determine the moment of the fracture for each ramus.

All these tests were recorded at a 10 kHz sampling rate.

Only one impact was delivered on the acetabulum through the metallic sphere. The choice of a single impact on the acetabulum was deduced from static tests. The stiffness of the pelvic ring in side loading, at least twice than those of the iliac wing, represents the major stiffness of the pelvic ring. Previous cadavers tests presented elsewhere, for which a double pelvis impactor was used [10], confirmed this difference of stiffness.

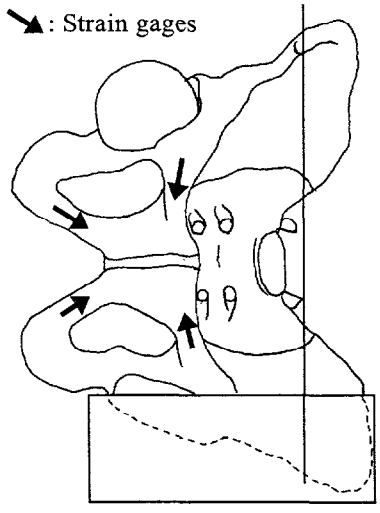

Figure 13 : positioning of the pelvis and location of the strain gauges.

Twelve pelvic bones were tested. They were provided from fresh cadavers through the department of anatomy of the "Faculté des Saints Pères" in Paris. Five of them were male specimens. The age ranged from 62 to 81 (mean 70 years). Metastasis or a long period of bed rest did not damage those cadaver bones. They were all stored at -18 °C before tests. A careful dissection kept undamaged the ligaments, especially posterior ligaments.

	Mass	Volume	Density
Mean	1240	1060	1.17
Min	870	750	1.1
Max	1480	1350	1.25

Table 4 : Main characteristics of the dynamic pelves.

A geometrical acquisition was also carried out on each tested pelvis using a 3D-measuring device, as described for static tests. X-rays for each pelvis were also taken to archive an image and to be sure that a previous fracture or metastasis did not damage the pelvis.

For the isolated pelvic bone, the impact energy was calculated to reach 30 Joules. This value was deduced from static tests, and represents the mean energy to obtain ramus fractures. The falling mass was adjusted to 3.68 kg, and the height calculated for an impact speed close to 4 m/s.

After each test, the pelvis was subjected to a careful observation in order to document the injuries. X-rays (antero-posterior, oblique and lateral) were taken and archived. They will be useful to compare the real life data with the experimental results.

RESULTS

Each pelvis was tested only once. 2 of them were intact after the impact. The 10 others exhibited a great variety of fractures from a single pubic ramus fracture to the complete pelvic crush. This first observation enabled us to confirm that the energy level was well chosen in order to approach the fracture threshold of the pelvis. These fractures, when occurring, were similar to those observed in the previous accidental study or in the literature. They are described in Appendix 6 and summarized in Table 5.

Fractures of one or two pubic ramus	4
Fractures of pubic ramus associated with posterior fracture (sacrum)	4
No fracture	2
Fractures of ilio pubic ramus extended to the acetabulum	1
Fractures of three or four pubic ramus	1

Table 5 : experimental results in terms of produced fractures.

Only pelves, which sustained posterior and anterior fractures, exhibited a high permanent displacement, always exceeding 10 mm (the maximum being over 70 mm). Pelves exhibiting only pubic fractures presented no or low permanent displacement after the test (less than 5 mm).

For the purpose of analysis, 3 groups were constituted: the first one without any fracture (2 pelves), the second one with only anterior fractures (6 pelves) and the last one with both anterior and posterior fractures (4 pelves).

One the other hand, the behavior curves were correlated to the three groups (Figure 14). Typical aspects were observed. The group without fracture is characterized by a high peak force and a displacement less than 5 mm, while the group of crushed pelves presented a high displacement with a low peak force.

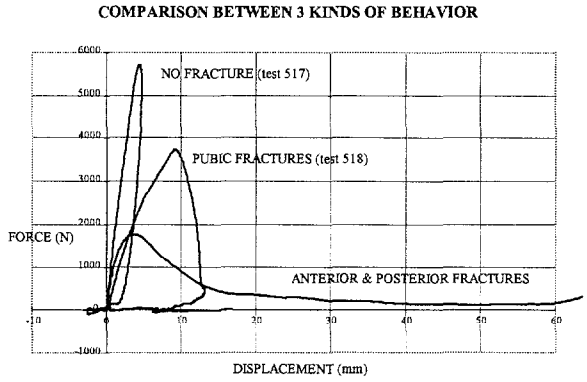

Figure 14 : behavior's patterns of the tested pelvic bones.

When a fracture was observed, the maximum force did not occur simultaneously with the maximum displacement. Actually, displacements at the instant of first fracture never exceeded 10 mm. Posterior injuries always occurred after anterior fractures. No significant correlation was found between force max and displacement at the moment of Force max. Complete data are reported in Appendix 6

Maximum force and maximum displacement for each test are summarized in the following graph (Figure 15). Three areas can be determined, and related to the anatomical damages, as defined before.

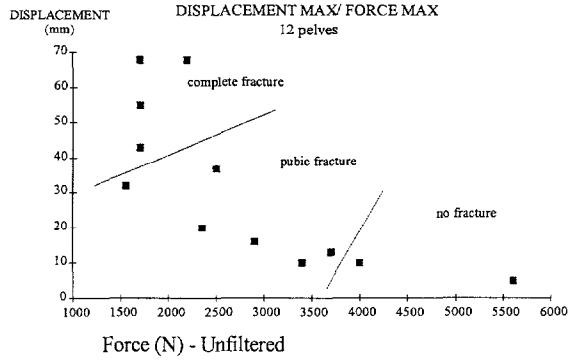

Figure 15 : classification of the pelves with regard to the ratio between the maximum displacement and the maximum force.

Data obtained from strain gages were also examined (Figure 16). The strain gages were oriented along the main axis of each ramus. A high range of responses was

observed. Right and left ilio pubic rami exhibited symmetrical signal during the impact, from 0.2 % for tests without pubic fracture to 1.2 % for tests with pubic fracture. For the ischial gages, the lowest value reached 0.1 % and never exceeded 0.8 %. It was assumed that the maximum of the strain curve was contemporaneous with the beginning of the rupture of the bony structure. A more detailed analysis still remains to be done in order to classify, when multiple fractures occurred, the order of occurrence of the different injuries.

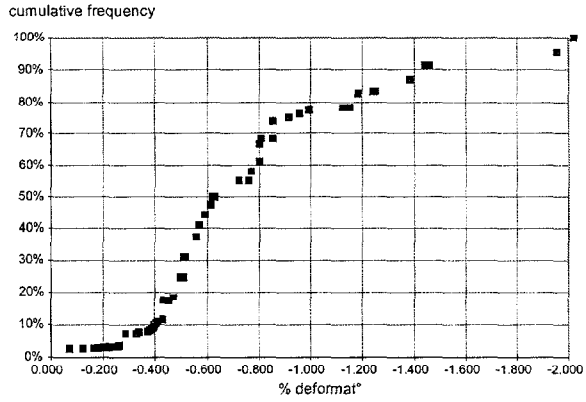

Figure 16 : Cumulative frequency of maximum strain for each pubic ramus

HISTOLOGICAL STUDY

Complementary studies were carried out in order to correlate the response of the pelvis with other parameters: geometry, bone mineral content and thickness of the cortical bone. A first approach was achieved for the static pelves, for which the bone mineral content was studied. The histological characterization of the specimens was obtained after inclusion in a polyester plaster. Each pelvis was sliced parallel to a reference plane (Figure 17) based on the foramen superior. Sixteen to 20 slices were obtained, according to the height of each pelvis. The thickness of the cortical bone was studied, and the mineral content of each slice determined by calcination. This method enabled us to access the overall mineral content as well as the mineral content of the sacrum, the iliac wing or the pubic rami. Furthermore, the mineralization of each ischio-pubic ramus by its length was calculated as an index (C/L) for the analysis.

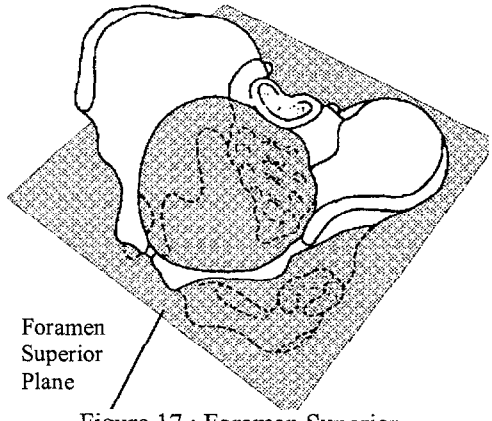

Figure 17 : Foramen Superior

A multiple regression analysis, including geometrical, mechanical and histological parameters, was performed with the results of the previous static tests.

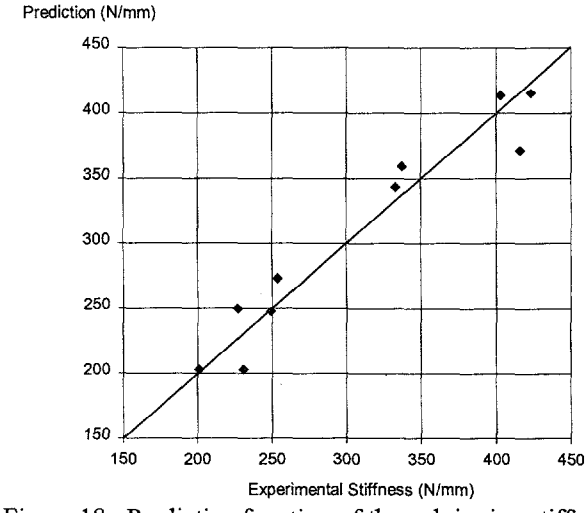

Figure 18 : Predictive fonction of the pelvic ring stiffness

A predictive fonction of the pelvic ring stiffness was first found, with only 3 parameters, with a R-squared, ajusted for degrees of freedom, up to 90 % (Figure 18):

SPR = 619.71 + 0.95*M - 0.29*V - 319.22*C/L

Where:

SPR = stiffness of the pelvic ring.

M = pelvic overall mineralization.

V = total volume.

C/L = index of ischio-pubic ramus mineralization.

Since the P-value is less than 0,01, there is a statistically significant relationship between these variables at the 99% confidence level. This relationship can be improved by adding the pelvis density as follows (Figure 19):

SPR = 115 + 416*D + 0.81*M - 0.24*V - 326.74*C/L

Where:

D = density of the pelvic bone.

The adjusted R-squared statistic for this enhanced fonction is 93,75 %.

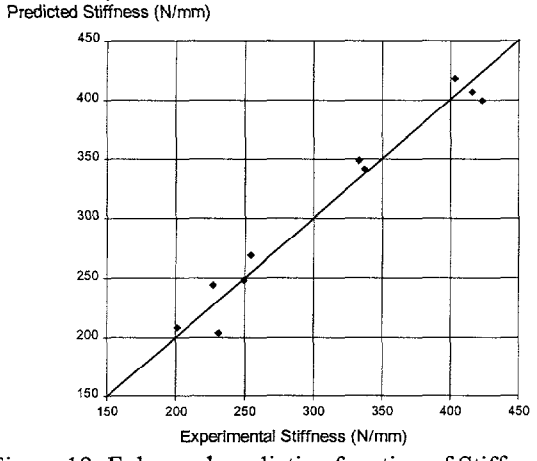

Figure 19: Enhanced predictive fonction of Stiffness

Another multiple regression analysis was performed, using the maximum force applied for a pelvic static fracture. First results, which are less significant than those from the stiffness, incited us to take into account 2 pelves (Figure 20). The first one is the female specimen, while the second is a 47-year-old specimen. Since variables as " age " and " gender " could be explained by others parameters such as thickness of the cortical bone, or geometry, for example, experiments on a wider sample are necessary to conclude.

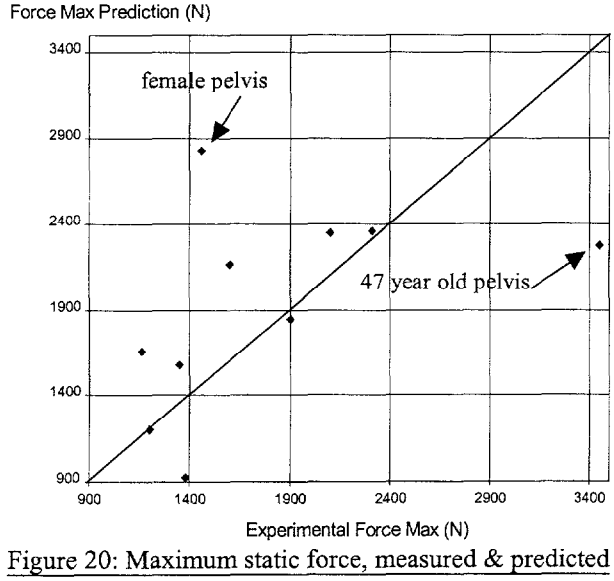

Figure 20: Maximum static force, measured & predicted

DISCUSSION

Several points can be noted for the static tests. The following comments can be made regarding the biomechanical aspect of the pelvic static behavior:

1 - Fracture threshold levels are lower in this study than those reported for whole body tests, but could be compared to Cesari static tests [5].

2 - Both displacement curves and strain gages show the specific behavior of the pubic symphisis, which can explain the mechanism of fracture.

As far as the anatomical aspect is concerned, it should be noted that:

1 - There is a lack of posterior injuries (i.e. sacro iliac disjunction), and opposite fractures.

2 - These experimental fractures were not well detected by X-rays.

The low thickness of the cortical bone of the pubic rami in this series, as well as the slow loading of the structure, and the removal of the load when the measured force began to decrease, can explain these observations.

Finally, the specific behavior of the female specimen should incite to study the influence of male and female geometry on mechanical responses.

On the other hand, varied fractures obtained from the dynamic tests are consistent with those observed in real life accidents. It was checked that the boundary conditions did not influence the results. Indeed, no fractures were observed near the interface between the pelvic bone and the low melting point alloy. Furthermore, a finite element study, using a published model [24], enables us to simulate different boundary conditions. Three different cases were examined, as follows:

- Loading with a metallic sphere in the acetabulum and the same immobilization as in the experimental tests.
- Loading with a metallic sphere and immobilization of a sphere fitted to the symmetrical acetabulum.
- symmetrical loading with two spheres in the acetabula.

No significant differences were found between the simulation results, thus confirming that the chosen boundary conditions were well adapted to this test.

A great range of responses was observed for those 12 pelves tested with a constant energy of 30 Joules. Displacement, applied force, local strains and fracture threshold were obtained. Applied force, from 1550 to 5600 N, was higher than those measured for static tests. Displacements at the moment of the fracture never exceeded 10 mm, which is close to those obtained for static tests. As those tests were performed with a constant energy, these results depend essentially on the geometrical characteristics and material properties.

Furthermore, more information was collected concerning both geometrical and histological data. It is expected that the most important parameters will be the thickness of the cortical bone and the bone mineral content, followed by the geometrical characteristics. A finite element simulation study is underway in order to assess the relative influence of these parameters and will be correlated with the results of the present study. These preliminary results, obtained from 12 pelvic bones tested on a drop tower, enable a first approach of an injury threshold on isolated pelvic bone (Figure 21). Displacement curves, force-time curves, as well as behavior curves from force and displacement, contributed to establish a tolerance level of the pelvic bone subjected to a side impact loading condition.

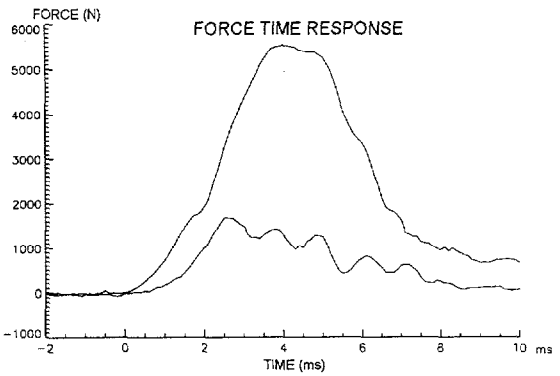

Figure 21 : experimental corridor.

CONCLUSION

This study enables us the assessment of the injuries sustained by a pelvis loaded in side impact conditions. The correlation between field accident studies and the experimentally reproduced injuries is a first step in the description of the injury mechanisms and of the tolerance of the pelvic bone. This knowledge is of particular interest for the optimization of protection devices and car structures as well as for the dimensioning of dummies or the definition of biofidel human models.

Complementary studies are yet underway in order to correlate the dynamic response of the pelvis with other parameters: geometry, bone mineral content and thickness of the cortical bone. In the course of this study, these parameters were planned to be documented. A wide geometrical database is now available and will be soon presented. The histological characterization of the dynamic specimens is also underway. Those pieces of information will thus be available for all the tested specimens, and further analysis will enable to draw out some correlation between geometrical, mechanical and histological data.

The assessment of the protection level must be provided for vehicle occupants in terms of pelvic resistance. All these studies will provide quantitative information suitable for the assessment of the efficiency of side impact protection devices.

ACKNOWLEDGMENTS

We would like to thank here the MAIF (Mutuelle d'Assurances des Instituteurs de France) Foundation for its financial support.

REFERENCES

1. Association For The Advancement Of Automotive Medicine: Abbreviated Injury Scale Revision 1990

2. Chamouard F, Brun-Cassan F, Le Coz JY, Guillon F, Bouchard L: Simulation Of The Human Behavior In Lateral Impact, IRCOBI 1993 159-173

3. Cavanaugh JM, Walilko TJ, Malhotra A, Zhu Y, King AI: Biomechanichal Response And Injury Tolerance Of The Pelvis In Twelve Sled Side Impacts, STAPP Conference 1990 1-12 (SAE 902305)

4. Cesari D, Ramet M, Clair P-Y: Evaluation Of Pelvic Fracture Tolerance In Side Impact, STAPP Conference 1980 231-253

5. Cesari D, Ramet M: Pelvic Tolerance And Protection Criteria In Side Impact STAPP Conference 1982 145-154 (SAE 821159)

6. Cesari D, Bouquet R Zac R: A New Pelvis Design For The European Side Impact Dummy, Stapp Conference 1984 1-11 (SAE 841650)

7. Dejeammes N: Fractures Du Bassin Au Cours Des Chocs Latéraux Automobiles, Thèse De Médecine, Université Claude Bernard, Lyon, 1978

8. Dischinger PC Cushing BM, Kerns TJ: Injury Patterns Associated With Direction Of Impact: Drivers Admitted To Trauma Centers J Of Trauma 1993 Vol 35 N°3 454-459

9. Guillemot H, Skalli W, Lavaste F, Got C, Le Coz JY: Static Behavior of the Pelvic Bone under Side Loading Conditions, PLEI Conference, Washington DC, 1995.

10. Guillemot H, Besnault B, Robin S, Got C, Lavaste F, Le Coz JY, Lassau JP: Pelvic Injuries in Side Impact Collisions: A Field Accident Analysis and Dynamic Tests on Isolated Pelvic Bones, STAPP Conference 1997, Orlando, FL, 91-100 (SAE 973322).

11. Hartemann F, Thomas C, Foret-Bruno JY, Henry C, Fayon A, Tarriere C: Occupant Protection In Lateral Impacts STAPP Conference 1976 191-219

12. Kallieris D, Mattern R, Schmidt G, Eppinger RH: Quantification Of Side Impact Responses And Injuries, STAPP Conference 1981 329-366 (SAE 811009)

13. Lestina DC, Gloyns PF, Rattenburry SJ: Fatally Injured Occupants In Side Impact Crashes, ESV Conference 1991 Section 3 Technical Sessions 701-707

14. Lewis P R Jr, Molz F J, Schmidtke S Z, , A NASS-Based Investigation of Pelvic Injury within the Motor Vehicle Crash Environment, SAE 962419

15. Lister RD, Neilson ID: Protection Of Car Occupants Against Side Impacts, STAPP Conference 1969 39-60

16. Marcus JH, Morgan RM, Eppinger RH, Kallieris D, Mattern R, Schmidt G: Human Response To And Injury From Lateral Impact, STAPP Conference 1983 419-432 (SAE 831634)

17. Melvin J-W, Robbins D-H, Stalnaker R-L: Side Impact Response And Injury, 6th ESV Conference 1976 681-689

18. Mills PJ, Hobbs CA: The Probability Of Injury To Car Occupants In Frontal And Side Impacts, STAPP Conference 1984 223-235 (SAE 841652)

19. Nuscholtz GS, Alem NM, Melvin JW: Impact Response And Injury Of The Pelvis, STAPP Conference Proceedings 1982 103-144 (SAE 821160)

20. Nuscholtz GS, Kaiser PS: Experimental Data For Development Of Finite Element Models, National Highway Traffic Safety Administration, Final Technical Report Vol 3 Pelvis Dec 1985

21. Nuscholtz GS, Kaiser PS: Pelvic Stress J Of Biomechanics, 1986, Vol 19, N° 12, 1003-1014

22. Plummer J W, Bidez M W, Alonso J, Parametric Finite Element Studies of the Human Pelvis: The Influence of Load Magnitude and Duration on Pelvic Tolerance During Side Impact, SAE 962411

23. Ramet M, Cesari D: Experimental Study Of Pelvis Tolerance In Lateral Impact Ircobi 1978, 243-249

24. Renaudin F, Guillemot H, Lavaste F, Skalli W, Got C: Mechanical Behavior Of Pelvic Bone in Axial Loading, ISATA Conference, Oct 1993

25. Renaudin F, Guillemot H, Lavaste F, Skalli W: A 3D Finite Element Model Of Pelvis In Side Impact, STAPP Conference, Nov 1993

26. Reynolds HM, Snow CC, Young JW: Spatial Geometry of the Human Pelvis, Memorandum report, AAC-119-81-5

27. Tarriere C, Walfisch G, Fayon A, Rosey J-P: Synthesis of Human Tolerances Obtained From Lateral Impact Simulations 7th ESV Conference 1979 359-373

28. Viano DC: Biomechanical Responses And Injuries In Blunt Lateral Impact, STAPP Conference Proceedings 1989 113-142

29. Zhu JY, Cavanaugh JM, King AI: Pelvic Biomechanical Response and Padding Benefits in Side Impact Based on a Cadaveric Test Series, STAPP Conference 1993, SAE 933128.

APPENDIX

Number	S1	S2	S3	S4	S5	S6	S7	S8	S9	S10
Age(years)	63	?	57	61	70	72	63	86	86	47
Gender	M	M	M	M	M	M	F	M	M	M
Weight(kg)	66	?	72	?	77	55	90	60	90	130
Height(cm)	163	?	174	?	175	160	165	167	175	180
Storage	+4°C	-20°C	+4°C	+4°C	+4°C	+4°C	+4°C	+4°C	+4°C	+4°C

Appendix 1 : Characteristics of the 10 static pelves

	Loading on Iliac Wing up to 500 N					
	Anterior Inferior Iliac Spine			Pubic Symphisis		
displ. (mm)	dX	dY	dZ	dX	dY	dZ
Pelvis S1	1.7	2.0	2.8	0.2	0.7	0.4
Pelvis S2	3.1	2.6	3.7	0.1	0.2	-0.1
Pelvis S3	1.1	1.6	2.1	0.2	0.5	0.1
Pelvis S4	1.6	1.9	3.8	0.2	0.3	/
Pelvis S5	0.6	2.8	2.3	0.3	0.4	-0.2
Pelvis S6	1.8	7.5	5.8	0.8	0.8	1.2
Pelvis S7	3.6	11.8	10.8	2.2	2.7	2.5
Pelvis S8	1.1	5.9	4.7	0.6	0.8	/
Pelvis S9	0.2	3.4	2.9	0.1	0.1	/
Pelvis S10	0.5	4.6	3.3	0.1	0.6	0.6

Appendix 2 : Displacements for iliac tests up to 500 N

	Loading through Acetabulum up to 500 N					
	Anterior Inferior Iliac Spine			Pubic Symphisis		
displ. (mm)	dX	dY	dZ	dX	dY	dZ
Pelvis S1	0.5	1.2	-0.4	0.7	0.6	0.3
Pelvis S2	0.3	1.6	-0.8	0.4	0.4	-0.3
Pelvis S3	0.4	1.6	-2.1	0.8	0.9	-0.9
Pelvis S4	0.8	1.4	-1.0	0.8	0.6	/
Pelvis S5	2	1.7	-2	1.5	1.1	-1
Pelvis S6	1.3	2.1	-1.7	1.0	1.1	-0.6
Pelvis S7	2.4	2.5	-0.6	1.6	1.8	0.1
Pelvis S8	1.2	2.1	-1.3	1.0	1.0	/
Pelvis S9	0.5	1.8	-1.1	0.6	0.5	/
Pelvis S10	0.7	1.4	-0.4	0.5	0.7	-0.1

Appendix 3 : Displacements for acetabular tests up to 500 N

Pelvis number	Injuries
S1	Right Ilio & ischio-pubic rami + sacrum
S2	Right Ilio & ischio-pubic rami
S3	Right Ilio & ischio-pubic rami
S4	Right Ilio & ischio-pubic rami
S5	Right Ilio & ischio-pubic rami
S6	Right Ilio & ischio-pubic rami
S7	Right Ilio & ischio-pubic rami
S8	Right Ilio & ischio-pubic rami
S9	Right Ilio & ischio-pubic rami
S10	Right Ilio & ischio-pubic rami

Appendix 4 : Main results of the static tests

N°	D1	D2	D3	D4	D5	D6	D7	D8	D9	D10	D11	D12
Sexe	F	M	M	F	F	F	F	M	M	M	M	F
Age (years)	77	65	62	73	65	81	81	70	67	72	75	73
Pelv.Mass (g)	1100	1480	1320	870	1350	1090	1060	1460	1270	1160	1440	1270
Volume (cm3)	975	1350	1060	750	1100	960	850	1310	1130	1030	1190	1050

Appendix 5 : Main characteristics of the dynamic pelves

Pelvis number	F Max (N)	$d_{(F\ Max)}$ (mm)	D Max (mm)	Injuries
D1	2197	8	68	Ilio & ischio-pubic rami + sacrum
D2	2350	4	20	4 pubic rami
D3	5600	5	5	None
D4	1700	7	68	Ilio & ischio-pubic rami + sacrum
D5	3700	9	13	Ilio & ischio-pubic rami
D6	1700	7	43	Ilio & ischio-pubic rami + sacrum
D7	4000	8,5	10	None
D8	1550	9	32	Ilio pubic ramus
D9	2500	4	37	Ilio & ischio-pubic rami
D10	1700	4	55	Ilio & ischio-pubic rami + sacrum
D11	3400	5	10	Ilio (extented to acetabulum) & ischio-pubic rami
D12	2900	7	16	Ilio & ischio-pubic rami

Appendix 6 : Main results of the dynamic tests